Catal Lett (2009) 130:235–238
DOI 10.1007/s10562-009-9872-7

Selective Catalytic Reduction of NO by Ammonia on V_2O_5/TiO_2 Catalyst Prepared by Sol–Gel Method

Xin Zhang · Xiaogang Li · Junsheng Wu ·
Renchun Yang · Zhihua Zhang

Received: 13 December 2008 / Accepted: 19 January 2009 / Published online: 5 February 2009

Abstract V_2O_5/TiO_2 catalysts with various vanadia loadings were prepared using inorganic precursor of vanadium by sol–gel method, and characterized by XRF, XRD, BET, Raman spectra and XPS techniques. Results demonstrated that the catalyst with 6.17 wt% vanadia had a high activity in the temperature range from 180 to 450 °C at a gas hourly space velocity of 10,000 h^{-1} and the activity was affected by increasing the space velocity at the temperature below 270 °C. All the catalysts showed high activity in the different temperature range under tested conditions.

Keywords SCR · V_2O_5/TiO_2 · NH_3 · Sol–gel method

1 Introduction

The sol–gel process has been a method to prepare highly pure and homogeneous multicomponent metal oxides, such as V_2O_5/TiO_2 catalysts for the selective catalytic reduction (SCR) of NO by ammonia. Baraket [1] fabricated a sulfated TiO_2 (V_2O_5–SO_4^{2-}/TiO_2) catalyst with low vanadia loading (1 wt%), and found that the NO conversion exceeds 90% at temperature above 400 °C. Djerad et al. [2, 3] studied the effects of vanadia and tungsten loadings on the physical and chemical properties of V_2O_5–WO_3/TiO_2 catalysts and concluded that the vanadia content influences significantly the catalytic behavior. An increase of vanadia loading causes the sintering of TiO_2 support and aggregation of isolated vanadium ions, enhancing the activity in SCR reaction in a narrow temperature range of about 100 °C.

To date, the relevant studies in catalytic activity of V-incorporated catalysts have been focused on the interaction of tungsten and sulfate ions with vanadia species and the resultant effects on SCR reaction. There has been limited work investigating the synergism of vanadia and titania on NO conversion.

In this work, V_2O_5/TiO_2 catalysts with various V loadings were prepared using inorganic precursor (vanadium oxalate solution) by sol–gel method. The interaction of vanadia and titania and the resultant effects on the structure of catalysts and NO conversion were characterized and discussed.

2 Experimental

2.1 Catalyst Preparation

All chemicals used in this work were in analytical reagent. The typical procedure to prepare V_2O_5/TiO_2 catalyst was shown as follows. 1.85 g hexadecylaminee (HDA) was dissolved in 9 g anhydrous ethanol, and nitric acid was added to adjust solution pH to 4. The mixture was stirred until the surfactant was completely dissolved. 6.80 g Tetrabutylorthotitanate (TBOT) was then added, and the solution was stirred until a transparent solution A was obtained.

Deionized water, 2 mol/L saturated vanadium oxalate solution and 4.60 g anhydrous ethanol was mixed, and

X. Zhang · X. Li (✉) · J. Wu · R. Yang · Z. Zhang
School of Material Science and Engineering,
University of Science and Technology Beijing,
100083 Beijing, China
e-mail: lixiaogang99@263.net

Present Address:
Z. Zhang
PetroChina Daqing Petrochemical Research Center,
163714 Daqing, China

nitric acid was added to adjust the pH value to 1.5. The mixture was stirred for 20 min and the solution B was obtained. The solution B was then slowly dripped into solution A, followed by vigorous stirring. Finally, a solution with pH of 2 was obtained and changed to gelatin gradually. The molar composition of the resultant gelatin was TBOT:HDA:H_2O:Ethanol = 1:0.5:3:15. After ageing at 80 °C for 72 h, the wet gelatin was dried in an oven at 80 °C for another 72 h. Finally, the catalyst powder was collected after it was calcined in a furnace at 250 °C for 2 h and then at 450 °C for another 2 h.

2.2 Characterization of Catalysts

The chemical compositions of catalysts were measured by Model 1800 X-ray fluorescence (XRF) analyzer (Japan). The specific surface area of catalyst was determined by nitrogen adsorption/desorption isotherms at −196 °C using an autosorb 1C apparatus (Quantachrome Instruments Co., USA). X-ray diffraction (XRD) was conducted through a X' Pert PRO MPD X-ray diffractometer (PANalytical Co. Holand). Cu Kα radiation ($\lambda = 1.5415$Å) was utilized as an X-ray gun operated at 40 kV and 40 mA. Diffraction patterns were obtained within the range of 2θ (10°–90°) at a scanning rate of 6° min^{-1}. Raman spectra were measured with a Nicolet Almega XR spectrometer with 632 nm line of Ar ion laser as excitation source under ambient condition. X-ray photoelectron spectroscopy (XPS) measurement was performed with a ESCALAB 250 (thermalfisher Co., USA) and an Mg anode (Mg Kα = 1,253.6 eV). The pressure in the main chamber was about 10^{-9} mbar. The C 1 s line was used as an internal standard to calibrate the binding energy. XPS measurements were carried out on samples after calcination only.

2.3 Activity Test

Catalyst activity was evaluated in a fixed bed flow reactor at atmospheric pressure. Typically, an approximate 4.5 cm^3 catalyst (40–200 mesh) was charged in a diameter of 12 mm stainless steel tube reactor. A feed gas stream containing NH_3 (1,000 ppm), NO (1,000 ppm), O_2 (5%) and N_2 (balance) was adjusted by mass flow controllers and introduced to the reactor with a total flow rate of 750 cm^3 min^{-1}, yielding a gas hourly space velocities (GHSV) of 10,000 h^{-1}. The test temperature was monitored and controlled by two K type thermocouples located on the top and the bottom of catalyst bed. Analysis of NO concentration was carried out using a Testo 350Xl (Germany). The reaction system was kept for 30 min at each reaction temperature to reach a steady state before each test was performed.

3 Results and Discussion

3.1 Characterization of Catalysts

Table 1 shows the V_2O_5 content, phase composition, specific surface area (S_{BET}), pore volume (V_P) and mean pore diameter that are determined from the experimental pore size distribution by Barrett Joiner Halenda (BJH) method. All specific surface areas of the tested sample are larger than 100 m^2 g^{-1}, with the largest one of 118.5 m^2 g^{-1}. A narrow pore size distribution exists in catalysts and the pore dimension is mainly at 6–8 nm.

At calcination temperature of 450 °C, all samples are monophasic, and only anatase of TiO_2 ($2\theta = 25.3°$–38.48°) is detected. No rutile phase was detected in the catalyst powders (Fig. 1). Moreover, no V_2O_5 crystallites were detected even at 6.17 wt% V_2O_5 content. It is probably attributed to the fact that vanadium oxides particles are present in scarce amount. Simultaneously, vanadium is well highly dispersed as isolated VO_X species [4] and has entered into the TiO_2 crystal framework.

The surface structure of vanadium on catalysts was examined by Raman spectroscopy, as shown in Fig. 2. It is generally acknowledged that the band around 1,030 cm^{-1} is associated with V=O bridge of monomeric VO_X [5–7], and the band around 920–940 cm^{-1} with V–O–V bridge of polymeric VO_X species [8–11]. The present result shows that only the peak around 1,030 cm^{-1} was observed, Therefore, vanadium in the two samples exists probably as V=O bridge of monomeric VO_X.

To identify the state of vanadium on the surface of TiO_2, the samples of CAT-1 and CAT-4 were examined by X-ray photoelectron spectroscopy (XPS). No peak of V 2p3/2 line at binding energy from 513 to 519 eV was observed in CAT-1, as shown in Fig. 3a. It is due to the fact that there was only 0.45% vanadium that was well dispersed and

Table 1 Morphological properties

Catalyst	V_2O_5 content (wt%)	Phase	S_{BET} (m^2 g^{-1})	V_P (cc g^{-1})	D_P (nm)
CAT-1	0.45	Anatase	111.80	0.17	5.95
CAT-2	1.15	Anatase	107.10	0.17	6.34
CAT-3	3.15	Anatase	101.50	0.19	7.34
CAT-4	6.17	Anatase	118.50	0.24	8.16

D_P pore diameter; V_P pore volume

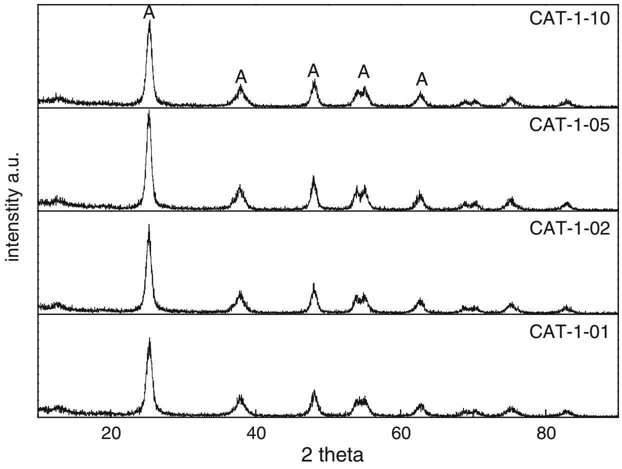

Fig. 1 X-ray diffraction pattern of solids catalyst

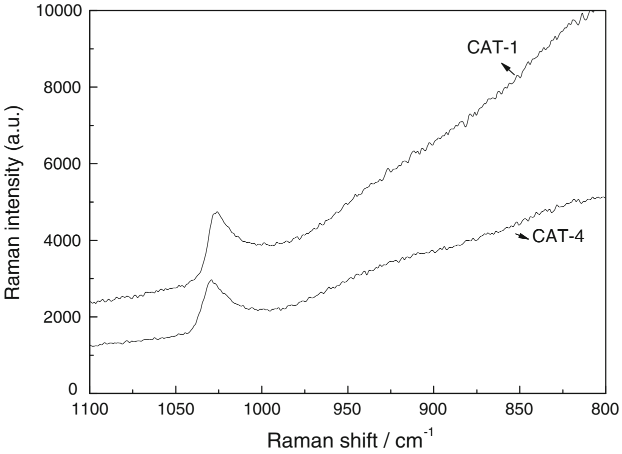

Fig. 2 Raman spectra of CAT-1 and CAT-4

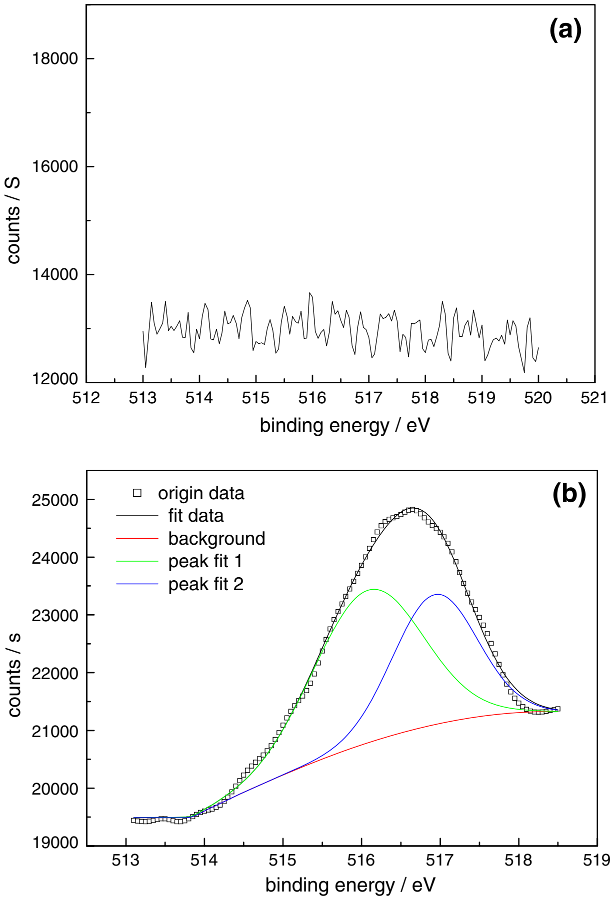

Fig. 3 XPS spectra of V 2p3/2 of the samples. **a** CAT-1; **b** CAT-4

entered into TiO_2 support. The spectrum of CAT-4 is shown in Fig. 3b, where the V 2p3/2 line at binding energy of 516.9 and 516.3 eV indicates that vanadium existing on the surface is in V^{5+} and V^{4+} oxidation state [1, 12]. According to calculating the area of XPS peak fitting, the ratio of V^{5+} and V^{+4} oxidation state is about 0.45:0.55.

3.2 Activity Tests for NO Reduction by NH3 Over V_2O_5/TiO_2 Catalysts

Figure 4 shows the NO conversion at various temperatures for SCR of NO by NH_3 over V_2O_5/TiO_2 catalysts with various V loadings. It is seen that, with the increase of V loading from 0.45 to 6.17%, the NO conversion is enhanced in the low temperature range (150–330 °C), and the characteristic temperature for the maximum NO conversion is shifted towards a lower temperature. For 6.17% V_2O_5/TiO_2, NO conversion is greater than 95% in a wide temperature range (180–450 °C).

Generally, with increasing vanadia loadings, more reactive sites are supplied. Consequently, the catalysts show a good activity in the wider temperature range. It was reported [1] that, at about 450 °C, the NO conversion of V_2O_5/TiO_2 catalyst with 1 wt% vanadia loading is greater than 90%. However, the present work identified a temperature of 360 °C for NO conversion. The catalysts developed in this work has a high specific surface area of about 110 $m^2\ g^{-1}$, a large porous volume of 0.17 cc g^{-1}, and a monomeric vanadia form, while the corresponding parameters for the reported catalyst are 22 $m^2\ g^{-1}$, 0.05 cc g^{-1} and a polymeric vanadia form, respectively.

The NO conversion on V_2O_5/TiO_2 catalyst prepared by sol–gel method, especially for the 6.17% V loading one, is similar to that on Mn–Ce/TiO_2 catalyst used at low temperature for removal of NO by ammonia [13], due to the high vanadium loading, the vanadium form of V=O bridge of monomeric VO_X V^{5+} and V^{4+} oxidation state. The reoxidation of the vanadium sites is the rate-limiting step in the SCR reaction at temperatures below 300 °C and V^{4+} species can speed up the rate-limiting step [14]. At the same time, higher surface area and larger porous volume can supply more reactive site.

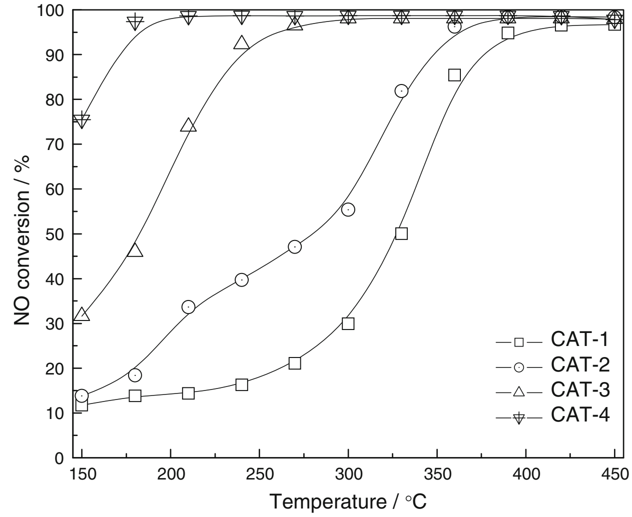

Fig. 4 Effect of vanadium loading on NO conversion. Reaction condition: NO 1,000 ppm, NH_3 1,000 ppm, O_2 5%, balance N_2, GHSV = 10,000 h^{-1}, total flow rate 750 cm^3 min^{-1}

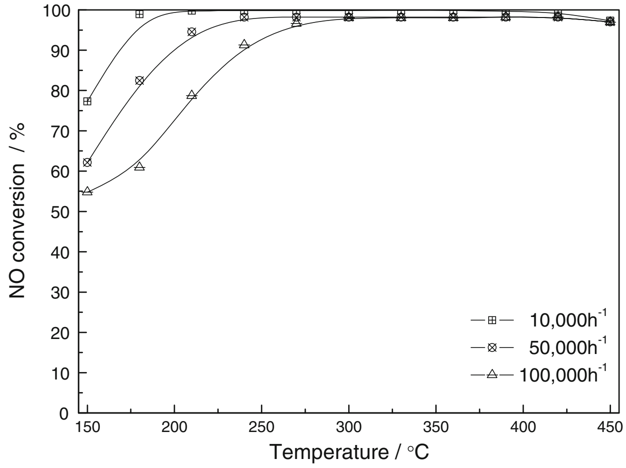

Fig. 5 Effect of space velocity on NO conversion over CAT-4. Reaction condition: NO 1,000 ppm, O_2 5%, balance N_2, total flow rate 750 cm^3 min^{-1}

3.3 Effect of GHSV Over 6.17% V_2O_5/TiO_2 for NO Reduction

The influence of GHSV on the NO conversion was studied by varying the GHSV over the 6.17% V_2O_5/TiO_2 catalyst. The catalyst activity decreases dramatically with the increasing space velocity from 10,000 to 100,000 h^{-1}, especially at the temperature below 270 °C. As shown in Fig. 5, for GHSV at 10,000 h^{-1}, the conversion was greater than 98% in the temperature range of 180−450 °C. At the GHSV of 50,000 h^{-1}, NO conversion was greater than 95% in the temperature range of 240–450 °C. Even at the GHSV of 100,000 h^{-1}, the conversion was greater than 95% in the temperature range of 300–450 °C. The results show that the 6.17% V_2O_5/TiO_2 catalyst is highly effective for NO conversion reduction within a wide range of GHSV.

4 Conclusions

The V_2O_5/TiO_2 catalysts prepared in the present work have a big special surface area, a narrow pore size distribution and a meso-structure. The vanadia was well dispersed by V=O bridge monolayer in V_2O_5/TiO_2 catalyst. V^{5+} and V^{4+} oxidization state was in 6.17 wt% vanadia loading catalyst. All V_2O_5/TiO_2 catalysts are highly active at a wide temperature range in presence of excess oxygen. The 6.17 wt% vanadia loading one is highly active and has a wide active temperature range (180–450 °C) and highly effective for NO conversion reduction within a wide range of gas hourly space velocity (10,000–100,000 h^{-1}).

Acknowledgments The authors are grateful for the financial support of Chinese National Programs for High Technology Research and Development (No. 2006AA05Z306).

References

1. Baraket L, Ghorbel A, Gange P (2007) Appl Catal B 72:37
2. Djerad S, Tifouti L, Crocoll M, Weisweiler W (2004) J Mol Catal A 208:257
3. Djerad S, Crocoll M, Kureti S, Tifouti L, Weisweiler W (2006) Catal Today 113:208
4. Zheng YJ, Jensen AD, Johnsson JE (2005) Appl Catal B 60:253
5. Choo ST, Lee YG, Nam IS, Ham SW, Lee JB (2000) Appl Catal A 200:177
6. Giakoumelou I, Fountzoula CH, Kordulis CH, Boghosian S (2000) Catal Today 73:255
7. Bulushev DA, Kiwi-Minsker L, Rainone F, Renken A (2002) J Catal 205:115
8. Went GT, Oyama ST, Bell AT (1990) J Phys Chem 94:4240
9. Magg N, Immaraporn B, Giorgi JB, Schroeder T, Baumer M, Dobler J, Wu ZL, Kondratenko E, Cherian M, Baerns M, Stair PC, Sauer J, Freund HJ (2004) J Catal 226:88
10. Wu Z, Stair PC, Rugmini S, Jackson SD (2007) J Phys Chem C 111:16460
11. Schimmoeller B, Schulz H, Ritter A, Reitzmann A, Kraushaar-Czarnetzki B, Baiker A, Pratsinis SE (2008) J Catal 256:74
12. Boudali LK, Ghorbel A, Grange P, Figueras F (2005) Appl Catal B 59:105
13. Qi GS, Yang RT (2003) Appl Catal B 44:217
14. Koebel M, Madia G, Raimondi F, Wokaun A (2002) J Catal 209:159